Supporting Information

A Catalytically-Driven Organometallic Molecular Motor

Ryan A. Pavlick, Krishna K. Dey, Andrew Sirjoosingh, Alan Benesi, and Ayusman Sen*

Department of Chemistry, The Pennsylvania State University, University Park, PA, 16802, (USA)

Calculation of diffusion coefficient

Samples were prepared using a constant concentration of catalyst 3mM (0.003 g) in a specific concentration of the substrate (ranging from 0.01M to 0.5M for diethyl diallylmalonate (DDM) and 0.05M to 1M for 1-pentene) in $CDCl_3$. Diffusion coefficients were calculated by using an 850 MHz NMR (Bruker) with a diffusion probe. The change in intensity was fit to the equation:

$$\ln\left(\frac{I}{I_0}\right) = -D\left(G\delta\gamma\right)^2\left(\Delta - \frac{\delta}{3} - \frac{\tau}{2}\right) \qquad (1)$$

Where I is the final resonance intensity, I_o is the initial intensity, D is the diffusion coefficient, G is the magnitude of the gradient, γ is the nuclear gyromagnetic ratio, δ is the gradient duration, τ is the gradient relaxation time, and Δ is the time between gradient pulses[1]. Each sample was run three times and multiple samples were averaged together and then corrected for changes in viscosity, Table S1, S2.

Table S1. Average diffusion coefficients, D, of Grubbs' catalyst in the presence of diethyl diallyl malonate (DDM).*

[DDM]	D ($\times 10^{-9} m^2/s$)	Std. Dev.	Viscosity (cP)	D ($\times 10^{-9} m^2/s$) corr. for visc.	Std. Dev. corr. for visc.
0M	0.662	0.018	0.400	0.662	0.018
0.01M	0.903	0.049	0.400	0.903	0.049
0.02M	0.770	0.01	0.405	0.768	0.008
0.05M	1.270	0.33	0.39	1.223	0.322
0.1M	1.250	0.203	0.467	1.458	0.237
0.5M	1.193	0.267	0.515	1.536	0.343
0.1M inhib.	0.701	0.026	0.467	0.818	0.030
0.5M inhib.	0.581	0.034	0.515	0.748	0.044
0.1M (completed)	0.672	0.072	0.467	0.784	0.084

*Measured at 295K in 0.6 ml of $CDCl_3$ in a AV-III-850MHz Bruker NMR with a diffusion probe. Catalyst concentration is 3mM and inhibitor concentration is 0.2M.

Table S2. Average diffusion coefficients, D, of Grubbs' catalyst measured in the presence of 1-pentene.*

[1-Pentene]	D ($\times 10^{-9} m^2/s$)	Std. Dev.	Viscosity (cP)	D ($\times 10^{-9} m^2/s$) corr. for visc.	Std. Dev. corr. for visc.
0M	0.66	0.02	0.33	0.66	0.02
0.05M	0.64	0.01	0.37	0.72	0.02
0.1M	0.86	0.12	0.35	0.91	0.12
0.5M	1.07	0.06	0.26	0.85	0.05
1M	0.81	0.03	0.26	0.64	0.02
0.05M inhib.	0.77	0.02	0.37	0.86	0.02
0.1M inhib.	0.81	0.07	0.35	0.86	0.08
0.5M inhib	0.81	0.02	0.26	0.64	0.02
1M inhib.	0.86	0.01	0.26	0.67	0.01
0.5M completed	0.86	0.04	0.26	0.68	0.03

* Measured at 295K in 0.6 ml of deuterated chloroform in a AV-III-850MHz Bruker NMR with a diffusion probe. Catalyst concentration is 3mM and inhibitor concentration is 0.2M.

The samples containing 1-pentene showed no significant increase in diffusion over the controls (with inhibitor and at equilibrium), Figure S1.

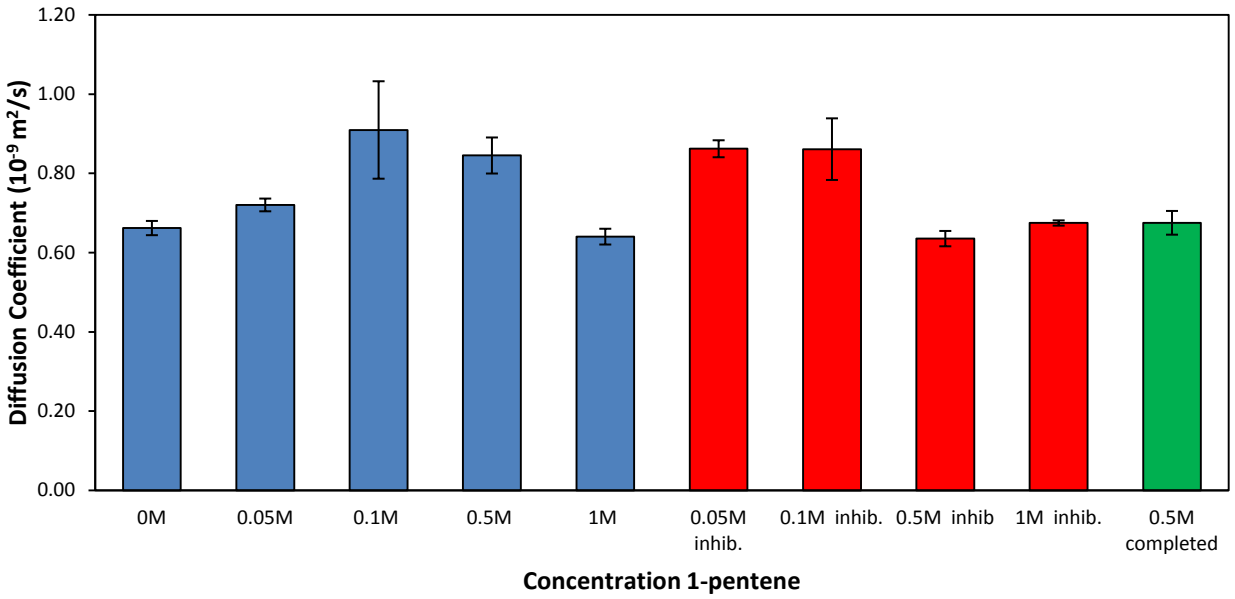

Fig S1. Diffusion coefficient at various concentrations of 1-pentene. Controls were run with inhibitor and after the reaction was completed. No significant change in diffusion was observed.

Measurement of turnover frequency (TOF)

While the rate constants are known in the literature [2], the turnover frequencies (TOF) were measured experimentally for all of the concentrations. The TOF were calculated from experiments run for 30 min. with NMR spectra taken every 10 min. The ethyl protons at the *1* position were standardized to integrate to 6 protons (Fig. S2). The integration value for the protons at position *3* was divided by 4 to find the percent of substrate left in solution. This was then related to a molar value since the starting amount of substrate was known. The moles of substrate left in solution was plotted versus time and a linear fit was used to extrapolate the reaction rate (mol sub./s). The velocity was then divided by the amount of catalyst in solution to obtain the TOF. The results are summarized in Table S3. It should be noted that all the measured TOFs are close to the values found in the literature [2]. There is a direct relationship between the TOF and diffusion coefficient (Figure S3).

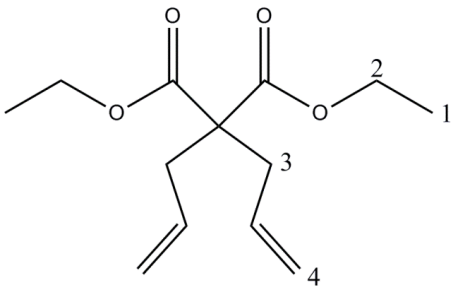

Fig. S2 Structure of diethyl diallyl malonate.

Table S3. TOF for the catalyst at varying concentrations of DDM.*

Conc.	TOF*
0M DDM	0
0.01M DDM	8.3E-04
0.02 DDM	1.5E-03
0.05M DDM	2.2E-03
0.1M DDM	4.2E-03
0.5M DDM	9.7E-03
0.5M 1-pentene	1.0E-02

*Measured in moles of substrate per mole of catalyst per sec.
Measured at 295K in $CDCl_3$ by a DPX-300MHz Bruker NMR.
Catalyst concentration is 3mM.

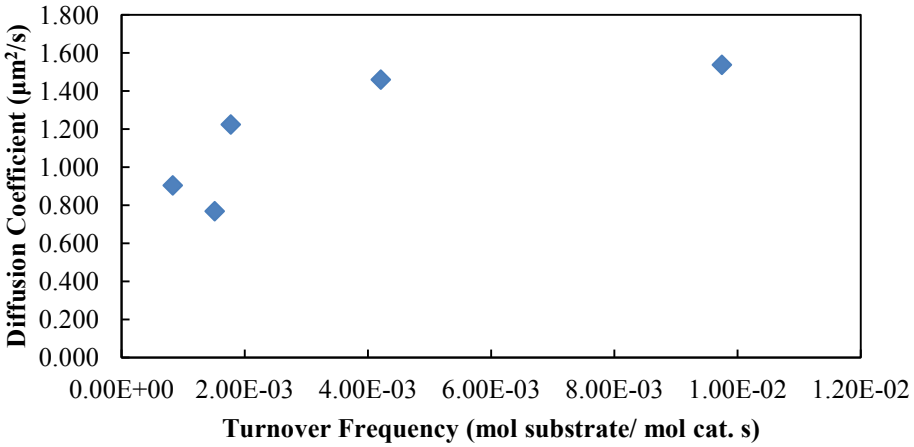

Fig. S3. Correlation between diffusion coefficient and turnover frequency

^{31}P NMR spectroscopy of the phosphine ligand

The ^{31}P NMR signal for the phosphine ligand was monitored in the absence and presence of substrates, Table S4. There is only one observable resonance whose position did not change significantly. Thus, we conclude that the dissociation of the phosphine from the metal center is slow compared to the NMR time scale.

Table S4. ^{31}P NMR data for Grubbs' 2nd generation catalyst in the absence and presence of substrates.*

Substrate	Shift (ppm)	Remarks
0 M DDM	29.05	
0.05MDDM	29.04	
0.1MDDM	29.02	
0.1MDDM	28.96	Inhibited
0.1MDDM	29.00	Completed
0.5MDDM	28.96	
0.5MDDM	28.96	15 min. later
0.5M 1-Pentene	29.03	

* Measured at 295K in 0.6ml $CDCl_3$ by a AV-360MHz Bruker NMR with a ^{31}P-NMR probe. Catalyst concentration is 3mM and Inhibitor concentration is 0.2M.

Efficiency of Energy Conversion:

Work done on a catalyst molecule due to a single turnover is given by $(6\pi\eta Ru).\Delta d$, where η is the coefficient of viscosity of the solvent (in N m^{-2} s), R is the radius of the catalyst molecule (in m), u is the velocity (in m/s) and d is the displacement of the molecule (in m) after the reaction.

$$\text{Rate of work done on the particle (in J/s)} = \frac{(6\pi\eta Ru).\Delta d}{\Delta t} = 6\pi\eta Ru^2 \qquad (1)$$

Considering N_{Cat} to be the number of moles of catalyst present in the system and ΔG to be the free energy of the system, then rate of production of free energy in the system is given by,

$$E = r \times \Delta G \times N_{Cat} \qquad (2)$$

Here, r is the turnover frequency measured in moles of substrate per mole of catalyst per sec.

If the efficiency of energy transformation is e, then the energy balance is,

$$6\pi\eta Ru^2 = e.E = e.(r \times \Delta G \times N_{Cat})$$

$$\text{or, } u^2 = \frac{e.(r \times \Delta G \times N_{Cat})}{6\pi\eta R} \qquad (3)$$

The rotational diffusion constant of a catalyst molecule is given by,

$$D_r = \frac{k_B T}{8\pi\eta R^3}$$

Here k_B Boltzmann constant and T is the temperature of the system.

The diffusion enhancement is [3],

$$\Delta D = \frac{u^2}{4D_r} = \frac{e.(r \times \Delta G \times N_{Cat}) \times 8\pi\eta R^3}{4 \times 6\pi\eta R \times k_B T} = \frac{1}{3}\frac{R^2}{k_B T} e.(r \times \Delta G \times N_{Cat})$$

$$\text{or, } e = \frac{3k_B T}{R^2 (r \times \Delta G \times N_{Cat})} \Delta D \qquad (4)$$

We take the values of different parameters as follows:

$k_B = 1.38\times10^{-23}$ J K^{-1}
$T = 298$ K
$R = 6\times10^{-10}$ m
$\Delta D = 9\times10^{-10}$ m^{2}s^{-1} (Maximum enhancement in diffusion observed)

$$r = 9.7\times10^{-3}\,\frac{(\text{moles of substrate})}{(\text{moles of catalyst}).\ \text{s}}$$

$$\Delta G = 2.2\ \frac{\text{kcal}}{\text{moles of substrate}} = 9.21\ \text{x}10^{3}\ \frac{\text{J}}{\text{moles of substrate}}$$

$N_{Cat} = 3.6\times10^{-5}$ moles

From Eq. (4) we then have: $e = 9.31\text{x}10^{-9}$

Therefore, efficiency of energy conversion of this system is $9.31\text{x}10^{-7}$ %

Density functional theory calculations of molecular volume, radius and energetics

Computational calculations were performed using Gaussian 09 [4]. Geometry optimizations of the ruthenium-containing species were performed using density functional theory (DFT) with the M06-2X functional [5] and the def2-SVP basis set [6,7]. This functional has been shown to perform reliably for this class of catalysts with respect to geometries and thermochemical calculations [8]. Molecular volumes of the optimized species at each step in the catalytic cycle (Figure S4) were calculated from the volume contained within a contour of 0.001 electrons/bohr of electronic density at the M06-2X/SVP level (Table S5). Geometry optimizations of the CM and RCM reactants and products were performed using DFT with the M06-2X functional and the 6-311++G** basis set [9]. Geometries of the solvated species were optimized in solution using the conductor-like polarizable continuum model (C-PCM) method [10,11] with ε=4.711300 and ε_∞=2.090627. Analytic frequency calculations were performed on the optimized structures (with appropriate solvation) in order to calculate the relevant thermochemical quantities at 298K at the M06-2X/6-311++G** level. The enthalpies and free energies of the CM reaction calculated using DFT were found to be similar to corresponding MP2/6-311++G** calculations.

For ring closing metathesis the enthalpy of reaction was 7.9 kcal/mol and the free energy of reaction was -2.2 kcal/mol. For cross metathesis (Z-4-octene product) the enthalpy of reaction was 2.2 kcal/mol and the free energy of reaction was -3.7 kcal/mol. For cross metathesis (E-4-octene product) the enthalpy of reaction was 3.4 kcal/mol and the free energy of reaction was -2.6 kcal/mol.

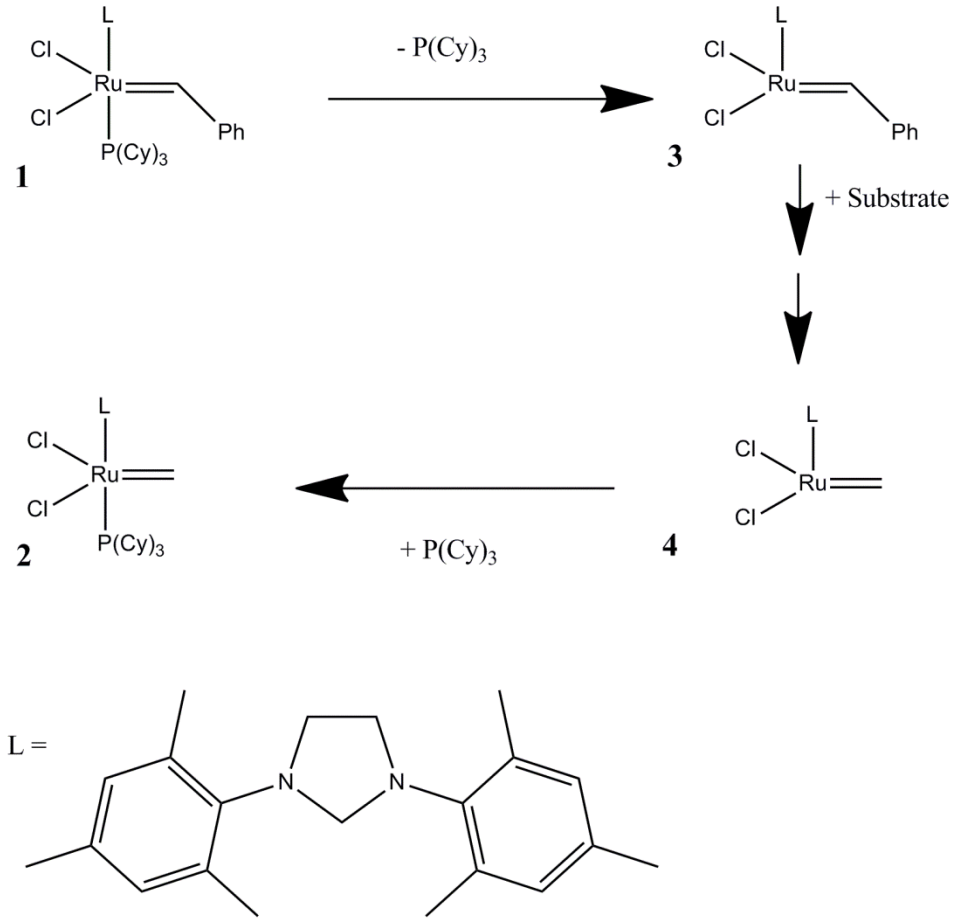

Fig S4. Structural changes to the catalyst molecule during the catalytic cycle

Table S5. Calculated effective radii from DFT of various intermediates.

Structure	System	Molecular volume ($Å^3$/mol)	Effective Radius from Volume (Å)	Difference (%)
1	$(H_2IMes)(PCy_3)Cl_2Ru=CHPh$	989.9230	6.18	-
2	$(H_2IMes)(PCy_3)Cl_2Ru=CH_2$	920.5719	6.03	2.4
3	$(H_2IMes)Cl_2Ru=CHPh$	580.7381	5.18	16.2
4	$(H_2IMes)Cl_2Ru=CH_2$	506.0585	4.94	20.1

References

[1] D.Wu, A. Chen, C. S. Johnson, *J. Magnetic Resonance Series A.* 1995, **115**, 260.

[2] M.S. Sanford, J. A. Love, R. H. Grubbs, *J. Am. Chem. Soc.***2001**, *123*, 6543 - 6554. ; S. Booyens, A. Roodt, O. F. Wendt, *J. Organometallic Chemistry.* 2007, **692**, 5508.

[3] J.R. Howse, R.A.L. Jones, A.J. Ryan, T. Gough, R. Vafabakhsh, R. Golestanian, *Phys. Rev. Lett*. 2007, **99**, 048102.

[4] M. J. Frisch, G. W. Trucks, H. B. Schlegel, G. E. Scuseria, M. A. Robb, J. R. Cheeseman, G. Scalmani, V. Barone, B. Mennucci, G. A. Petersson, H. Nakatsuji, M. Caricato, X. Li, H. P. Hratchian, A. F. Izmaylov, J. Bloino, G. Zheng, J. L. Sonnenberg, M. Hada, M. Ehara, K. Toyota, R. Fukuda, J. Hasegawa, M. Ishida, T. Nakajima, Y. Honda, O. Kitao, H. Nakai, T. Vreven, J. A. Montgomery, J. E. Peralta, F. Ogliaro, M. Bearpark, J. J. Heyd, E. Brothers, K. N. Kudin, V. N. Staroverov, R. Kobayashi, J. Normand, K. Raghavachari, A. Rendell, J. C. Burant, S. S. Iyengar, J. Tomasi, M. Cossi, N. Rega, J. M. Millam, M. Klene, J. E. Knox, J. B. Cross, V. Bakken, C. Adamo, J. Jaramillo, R. Gomperts, R. E. Stratmann, O. Yazyev, A. J. Austin, R. Cammi, C. Pomelli, J. W. Ochterski, R. L. Martin, K. Morokuma, V. G. Zakrzewski, G. A. Voth, P. Salvador, J. J. Dannenberg, S. Dapprich, A. D. Daniels, Farkas, J. B. Foresman, J. V. Ortiz, J. Cioslowski, and D. J. Fox, Gaussian 09, Revision B.01 (Wallingford CT, 2009).

[5] Y. Zhao, D. G. Truhlar, *Theor. Chem. Acc.***120**, 215 (2008).

[6] D. Andrae, U. Haussermann, M. Dolg, H. Stoll, H. Preuss, *Theor. Chim. Acta* 1990, **77**, 123.

[7] F. Weigend, R. Ahlrichs, *Phys. Chem. Chem. Phys.* 2005, **7**, 3297.

[8] H. Eshuis, F. Furche, *J. Phys. Chem. Lett.* 2011, **2**, 983.

[9] R. Krishnan, J. S. Binkley, R. Seeger, J. A. Pople, *J. Chem. Phys.* 1980, **72**, 650.

[10] V. Barone, M. Cossi, *J. Phys. Chem. A* 1998, **102**, 1995.

[11] M. Cossi, N. Rega, G. Scalmani, V. Barone, *J. Comput. Chem.* 2003, **24**, 669.